

Goldstone mode singularities in $O(n)$ models

J. Kaupužs^{1,2}, R.V.N. Melnik³, J. Rimšāns^{1,2}

¹ Institute of Mathematics and Computer Science, University of Latvia,
 29 Raiņa Boulevard, LV-1459 Riga, Latvia

² Institute of Mathematical Sciences and Information Technologies, University of Liepaja,
 14 Liela St., Liepaja LV-3401, Latvia

³ Wilfrid Laurier University, Waterloo, Ontario, Canada, N2L 3C5

Received July 3, 2012, in final form August 28, 2012

Monte Carlo (MC) analysis of the Goldstone mode singularities for the transverse and the longitudinal correlation functions, behaving as $G_{\perp}(\mathbf{k}) \simeq ak^{-\lambda_{\perp}}$ and $G_{\parallel}(\mathbf{k}) \simeq bk^{-\lambda_{\parallel}}$ in the ordered phase at $k \rightarrow 0$, is performed in the three-dimensional $O(n)$ models with $n = 2, 4, 10$. Our aim is to test some challenging theoretical predictions, according to which the exponents λ_{\perp} and λ_{\parallel} are non-trivial ($3/2 < \lambda_{\perp} < 2$ and $0 < \lambda_{\parallel} < 1$ in three dimensions) and the ratio bM^2/a^2 (where M is a spontaneous magnetization) is universal. The trivial standard-theoretical values are $\lambda_{\perp} = 2$ and $\lambda_{\parallel} = 1$. Our earlier MC analysis gives $\lambda_{\perp} = 1.955 \pm 0.020$ and λ_{\parallel} about 0.9 for the $O(4)$ model. A recent MC estimation of λ_{\parallel} , assuming corrections to scaling of the standard theory, yields $\lambda_{\parallel} = 0.69 \pm 0.10$ for the $O(2)$ model. Currently, we have performed a similar MC estimation for the $O(10)$ model, yielding $\lambda_{\perp} = 1.9723(90)$. We have observed that the plot of the effective transverse exponent for the $O(4)$ model is systematically shifted down with respect to the same plot for the $O(10)$ model by $\Delta\lambda_{\perp} = 0.0121(52)$. It is consistent with the idea that $2 - \lambda_{\perp}$ decreases for large n and tends to zero at $n \rightarrow \infty$. We have also verified and confirmed the expected universality of bM^2/a^2 for the $O(4)$ model, where simulations at two different temperatures (couplings) have been performed.

Key words: Monte Carlo simulation, n -component vector models, correlation functions, Goldstone mode singularities

PACS: 05.10.Ln, 75.10.Hk, 05.50.+q

1. Introduction

Our work is devoted to the Monte Carlo (MC) investigation of the Goldstone mode effects in n -component vector-spin models ($O(n)$ models), which have $O(n)$ global rotational symmetry at zero external field \mathbf{h} . The Hamiltonian \mathcal{H} is given by

$$\frac{\mathcal{H}}{T} = -\beta \left(\sum_{\langle ij \rangle} \mathbf{s}_i \mathbf{s}_j + \sum_i \mathbf{h} \mathbf{s}_i \right), \quad (1.1)$$

where T is temperature, $\mathbf{s}_i \equiv \mathbf{s}(\mathbf{x}_i)$ is the n -component vector of unit length, i. e., the spin variable of the i -th lattice site with coordinate \mathbf{x}_i , and β is the coupling constant. The summation takes place over all nearest neighbors in the lattice with periodic boundary conditions.

The Fourier-transformed longitudinal and transverse correlation functions are

$$G_{\parallel}(\mathbf{k}) = N^{-1} \sum_{\mathbf{x}} \tilde{G}_{\parallel}(\mathbf{x}) e^{-i\mathbf{k}\mathbf{x}}, \quad (1.2)$$

$$G_{\perp}(\mathbf{k}) = N^{-1} \sum_{\mathbf{x}} \tilde{G}_{\perp}(\mathbf{x}) e^{-i\mathbf{k}\mathbf{x}}, \quad (1.3)$$

where $\tilde{G}_{\parallel}(\mathbf{x})$ and $\tilde{G}_{\perp}(\mathbf{x})$ are the corresponding two-point correlation functions in the coordinate space.

In the thermodynamic limit below the critical temperature (at $\beta > \beta_c$), the magnetization $M(h)$ and the correlation functions exhibit Goldstone mode power-law singularities:

$$M(h) - M(+0) \propto h^\rho \quad \text{at} \quad h \rightarrow 0, \quad (1.4)$$

$$G_\perp(\mathbf{k}) = a k^{-\lambda_\perp} \quad \text{at} \quad h = +0 \text{ and } k \rightarrow 0, \quad (1.5)$$

$$G_\parallel(\mathbf{k}) = b k^{-\lambda_\parallel} \quad \text{at} \quad h = +0 \text{ and } k \rightarrow 0, \quad (1.6)$$

where a and b are the amplitudes.

There exist different theoretical predictions for the values of the exponents in these expressions. In a series of theoretical works (e. g., [1–7]), it has been claimed that these exponents are exactly $\rho = 1/2$ at $d = 3$, $\lambda_\perp = 2$ and $\lambda_\parallel = 4 - d$. Here, d is the spatial dimensionality $2 < d < 4$. These theoretical approaches are further referred to as the standard theory.

More non-trivial universal values are expected according to [8], such that

$$d/2 < \lambda_\perp < 2, \quad (1.7)$$

$$\lambda_\parallel = 2\lambda_\perp - d, \quad (1.8)$$

$$\rho = (d/\lambda_\perp) - 1 \quad (1.9)$$

hold for $2 < d < 4$. These relations were obtained in [8] by analyzing self-consistent diagram equations for correlation functions without cutting the perturbation series. As introduced in [9, 10], we will call this approach the GFD (grouping of Feynman diagrams) theory. Apart from the mathematical analysis, certain physical arguments were also provided [8] to show that $\lambda_\perp = 2$ could not be the correct result for the XY model ($n = 2$) within $2 < d < 4$.

Several MC simulations were performed in the past [11–14] to verify the compatibility of MC data with some standard-theoretical expressions, where the exponents are fixed. In recent years, we performed a series of accurate MC simulations [10, 15, 16] for remarkably larger lattices than previously with an aim to reexamine the theoretical predictions by evaluating the exponents in (1.7)–(1.9). In particular, lattices of the linear sizes $L \leq 512$ for $n = 2$ and $L \leq 350$ for $n = 4$ were simulated in our papers [10, 15] and [16], respectively. These L values remarkably exceed the largest sizes simulated by other authors, i. e., $L = 160$ for $n = 2$ in [13] and $L = 120$ for $n = 4$ in [12, 14]. In the current work, the $O(10)$ model is simulated up to $L = 384$.

The relations (1.7) and (1.8) are consistent with MC simulation results for the 3D $O(4)$ model [16], where an estimate $\lambda_\perp = 1.955 \pm 0.020$ was found. It was also stated that the behavior of the longitudinal correlation function is well consistent with λ_\parallel about 0.9 rather than with the standard-theoretical value $\lambda_\parallel = 1$. According to (1.9), we have $1/2 < \rho < 1$ in three dimensions. It is consistent with the MC estimate $\rho = 0.555(17)$ for the 3D XY model [15], which corresponds to $\lambda_\perp = 1.929(21)$ according to (1.9). A clear MC evidence that the behavior of $G_\parallel(\mathbf{k})$ is not quite consistent with the standard-theoretical predictions has been recently provided [10], where an estimate $\lambda_\parallel = 0.69 \pm 0.10$ has been obtained for the 3D XY (i. e., 3D $O(2)$) model (at $\beta = 0.55$), assuming corrections to scaling of the standard theory.

In the actual study, we have extended our MC simulations and analysis to include the $n = 10$ case and to test the n -dependence of the exponents. Apart from the exponents, we have performed here an extended analysis of the $O(4)$ model to verify the expected universality of the ratio bM^2/a^2 [8], where $M \equiv M(+0)$ is the spontaneous magnetization, a and b are the amplitudes in (1.5) and (1.6).

2. Simulation results

We simulated the 3D $O(10)$ model by a modified Wolff cluster algorithm, used also in [15, 16], and evaluated the Fourier-transformed correlation functions by techniques described in [16]. The standard Wolff cluster algorithm [17] was modified to enable simulations at nonzero external field \mathbf{h} . Simple cubic lattices of the linear size up to $L = 384$ were simulated at $\beta = 3$ and $h = |\mathbf{h}| = h_{\min}, 2h_{\min}, 4h_{\min}$, where $h_{\min} = 0.00021875$. The coupling constant $\beta = 3$ corresponds to the ordered phase, since the spontaneous magnetization $M(+0)$ is about 0.467 in this case — see section 5 for details. This value of $M(+0)$ is comparable with those for the $O(2)$ and $O(4)$ models in our previous MC simulations [15, 16]. The simulation

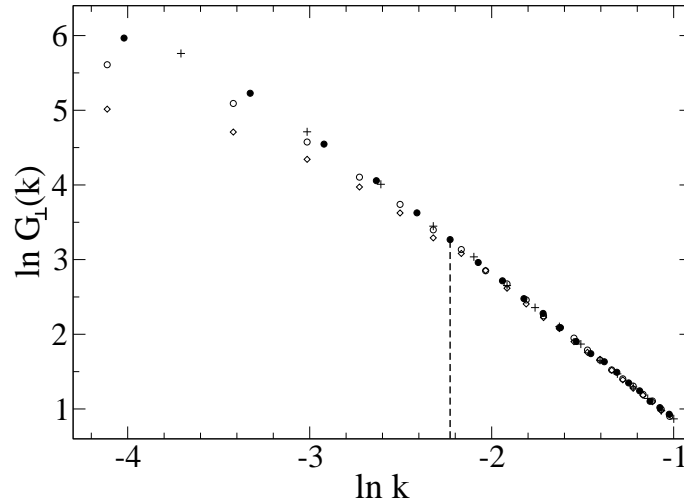


Figure 1. Log-log plots of the transverse correlation function $G_{\perp}(\mathbf{k})$ at $h = h_{\min} = 0.00021875$ and $L = 350$ (solid circles), $h = h_{\min}$ and $L = 256$ (pluses), $h = 2h_{\min}$ and $L = 384$ (empty circles), as well as at $h = 4h_{\min}$ and $L = 384$ (empty diamonds). Statistical errors are about the symbol size or smaller. The lower value k^* of the wave vector magnitude, used in estimations of the exponent λ_{\perp} , is indicated by a vertical dashed line.

results for the correlation functions $G_{\perp}(\mathbf{k})$ and $G_{\parallel}(\mathbf{k})$ in the $\langle 100 \rangle$ crystallographic direction at the three values of h and different sizes L are illustrated in figures 1 and 2. It is important for an estimation of the exponents λ_{\perp} and λ_{\parallel} to ensure that the finite-size as well as finite- h effects are small. This condition is satisfied for $k > k^*$, where the values of k^* are indicated in the figures by vertical dashed lines.

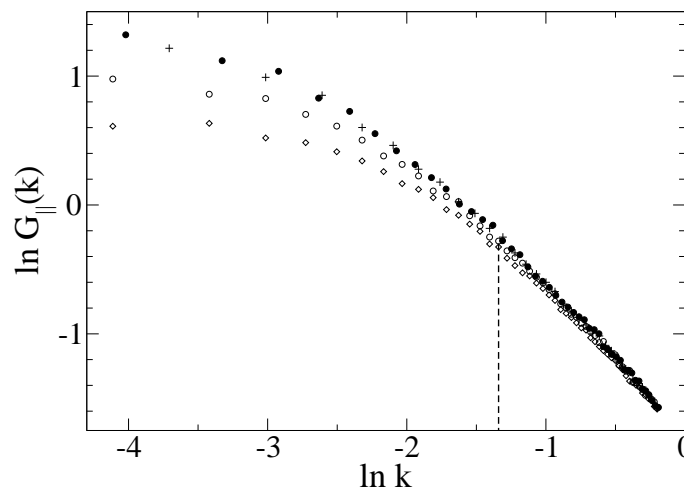


Figure 2. Log-log plots of the longitudinal correlation function $G_{\parallel}(\mathbf{k})$ at $h = h_{\min} = 0.00021875$ and $L = 350$ (solid circles), $h = h_{\min}$ and $L = 256$ (pluses), $h = 2h_{\min}$ and $L = 384$ (empty circles), as well as at $h = 4h_{\min}$ and $L = 384$ (empty diamonds). Statistical errors are about the symbol size. The lower value k^* of the wave vector magnitude, used in estimations of the exponent λ_{\parallel} , is indicated by a vertical dashed line.

3. Estimation of the exponents

Here we estimate the exponents λ_{\perp} and λ_{\parallel} , describing the behavior of the correlation functions in the limit $k \rightarrow 0$, $h \rightarrow 0$, $L \rightarrow \infty$, taking the limit $L \rightarrow \infty$ at first, followed by $h \rightarrow 0$. For this purpose, first we find good approximations of the effective exponents at $h \rightarrow 0$, $L \rightarrow \infty$, and then fit these k -dependent effective exponents to evaluate their asymptotic values at $k \rightarrow 0$. By comparing the simulation results for different L and h , we conclude that the largest- L and smallest- h data for $k > k^*$ with a good enough accuracy correspond to the thermodynamic limit at $h = +0$, i. e., $h \rightarrow 0$, $L \rightarrow \infty$. We have tested this precisely by looking how the estimates of the effective exponents depend on L and h . This method of analysis was applied in [10, 16]. The effective transverse exponent $\lambda_{\text{eff}}(k)$ for the $O(4)$ model was evaluated in [16] from the slope of the $\ln G_{\perp}(\mathbf{k})$ vs $\ln k$ plot within $[k, 4k]$. Here we use a wider interval — $[k, 6k]$, because we have found that the $\lambda_{\text{eff}}(k)$ data in this case can be perfectly fit by a parabola

$$\lambda_{\text{eff}}(k) = \lambda_{\perp} + a_1 k + a_2 k^2, \quad (3.1)$$

the finite-size and finite- h effects being very small. The ansatz (3.1) is consistent with the general statement $\lim_{k \rightarrow 0} \lambda_{\text{eff}}(k) = \lambda_{\perp}$ (in the thermodynamic limit at $h = +0$) and with corrections to scaling of the standard theory, where the correlation functions are supplied with correction factors in the form of an expansion in powers of k^{4-d} and k^{d-2} [1, 5]. Some of the fit results are shown in figure 3. We have performed a series of fits at different sizes L for the smallest- h value $h = h_{\text{min}} = 0.00021875$. At the largest size $L = 350$ for this h , the effective exponent $\lambda_{\text{eff}}(k)$ was fit within $k \in [k_5, k_{25}]$, where $k_{\ell} = 2\pi\ell/350$ are the possible discrete values of k . Similar fit intervals were chosen for all L . These fits to (3.1) give us $\lambda_{\perp} = 1.9680(84)$ at $L = 128$, $\lambda_{\perp} = 1.9840(98)$ at $L = 192$, $\lambda_{\perp} = 1.9727(86)$ at $L = 256$ and $\lambda_{\perp} = 1.9723(90)$ at $L = 350$. As we can see, the finite-size effects are smaller than the statistical error bars. The $\lambda_{\text{eff}}(k)$ data for $L = 350$ and $L = 256$ at $h = h_{\text{min}}$ are shown in figure 3 by solid circles and exes, respectively. The corresponding fit curves lie practically on top of each other. Therefore, only that one for $L = 350$ is shown by solid line. The fit curves for $h = 2h_{\text{min}}$ and $h = 4h_{\text{min}}$ at $L = 384$ (the largest size) are also depicted here to see the finite- h effects. These fits give us $\lambda_{\perp} = 1.9251(86)$ at $h = 4h_{\text{min}}$ and $\lambda_{\perp} = 1.9666(91)$ at $h = 2h_{\text{min}}$. A rather fast convergence to the $h = +0$ limit is evident. According to this discussion, the fit result $\lambda_{\perp} = 1.9723(90)$, obtained at $h = h_{\text{min}}$ and $L = 350$, with a good accuracy corresponds to the thermodynamic limit at $h = +0$. Besides, the systematical errors due to finite-size and finite- h effects are probably smaller than the statistical error bars.

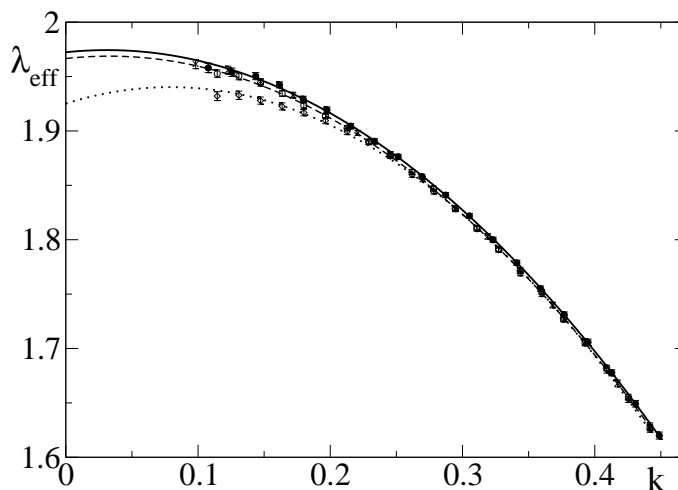


Figure 3. The transverse effective exponent $\lambda_{\text{eff}}(k)$, evaluated from the $\ln G_{\perp}(\mathbf{k})$ vs $\ln k$ fits within $[k, 6k]$ at $h = h_{\text{min}} = 0.00021875$ and $L = 350$ (solid circles), $h = h_{\text{min}}$ and $L = 256$ (exes), $h = 2h_{\text{min}}$ and $L = 384$ (empty circles), as well as at $h = 4h_{\text{min}}$ and $L = 384$ (empty diamonds). The fits to (3.1) of the largest- L data at $h = h_{\text{min}}$, $h = 2h_{\text{min}}$ and $h = 4h_{\text{min}}$ are shown by solid, dashed and dotted lines, respectively.

Another possible source of systematical errors is the existence of non-trivial corrections to scaling, which are not included in (3.1). These are corrections to scaling of the GFD theory [8], represented by an expansion in powers of $k^{2-\lambda_{\perp}}$, $k^{\lambda_{\perp}-\lambda_{\parallel}}$ and $k^{\lambda_{\parallel}}$. Nevertheless, the actual estimation, where only the standard-theoretical corrections have been included, is well justified as a test of consistency of the standard theory. The existence of a small correction-to-scaling exponent $2 - \lambda_{\perp}$ can make the extrapolation of the $\lambda_{\text{eff}}(k)$ plots unreliable. However, since the $\lambda_{\text{eff}}(k)$ data are really well described by a parabola, it might be true that the amplitude of such a correction term is small and the estimate $\lambda_{\perp} = 1.9723(90)$ is quite reasonable. In any case, this estimation shows a small deviation from the standard-theoretical picture, where (3.1) should hold at small enough k with $\lambda_{\perp} = 2$. This deviation can be indeed small at $n = 10$, since $\lambda_{\perp} \rightarrow 2$ is expected in the limit $n \rightarrow \infty$, corresponding to the known behavior of the spherical model [18].

We have also attempted to evaluate the longitudinal exponent λ_{\parallel} from the $G_{\parallel}(\mathbf{k})$ data within $k > k^*$, where k^* is indicated in figure 2 by a vertical dashed line. We have found that the longitudinal effective exponent, extracted from the data within $[k, 4k]$, can be perfectly approximated by a parabola. It leads to an estimate $\lambda_{\parallel} = 0.85 \pm 0.06$. The error bars indicated here include a statistical standard error as well as a systematical error due to finite- h effects. However, due to a rather large extrapolation gap (from ≈ 1.17 to ≈ 0.85), we consider this estimation as a preliminary one.

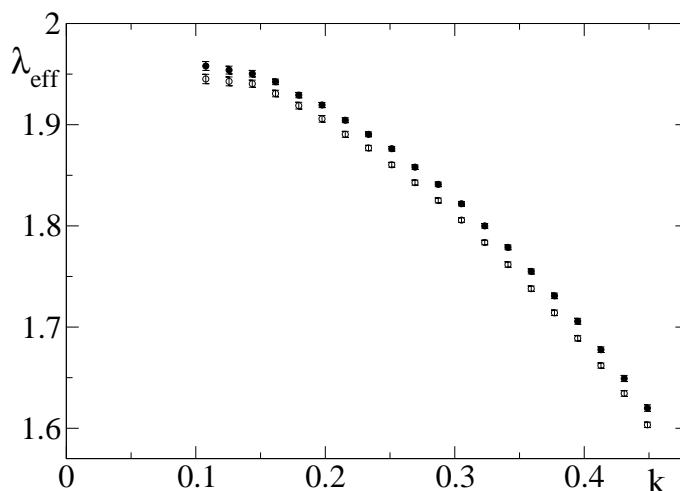


Figure 4. The plots of the transverse effective exponent $\lambda_{\text{eff}}(k)$, evaluated from the $\ln G_{\perp}(\mathbf{k})$ vs $\ln k$ fits within $[k, 6k]$. The results of the $O(10)$ model at $\beta = 3$ are shown by solid circles, whereas those of the $O(4)$ model at $\beta = 1.1$ — by empty circles.

We have reexamined the largest- L ($L = 350$) and smallest- h ($h = 0.0003125$) data of the $O(4)$ model [16] at $\beta = 1.1$ with an aim to evaluate the transverse effective exponent in the same way as for the $O(10)$ model. Like in the $n = 10$ case, we have verified that the thermodynamic limit at $h = +0$ is practically reached in this estimation. Besides, we have found a surprising similarity of the $\lambda_{\text{eff}}(k)$ plots, where the effective exponent in both cases was evaluated by fitting the $G_{\perp}(\mathbf{k})$ data within $[k, 6k]$ (fits within $[k, 4k]$ were used in [16]). As we can see from figure 4, the plot for the $O(4)$ model is systematically shifted down by an almost constant value relative to the same plot for the $O(10)$ model. This similarity might be partly caused by the fact that the values of spontaneous magnetization are rather similar in these two cases, i. e., $M \equiv M(+0) = 0.484475(48)$ for the $O(4)$ model at $\beta = 1.1$ and $M \approx 0.467$ (see section 5) for the $O(10)$ model at $\beta = 3$. The overall fit to (3.1) is less perfect for the $O(4)$ model as compared to the $O(10)$ model. However, the systematical shift between two plots is very well approximated by a constant value within the statistical error bars for the eight smallest k data points in figure 4. It yields an estimate $\Delta\lambda_{\perp} = (\lambda_{\perp})_{n=10} - (\lambda_{\perp})_{n=4} = 0.0121(52)$, where $(\lambda_{\perp})_{n=10}$ and $(\lambda_{\perp})_{n=4}$ are the values of λ_{\perp} in $n = 10$ and $n = 4$ cases. According to the behavior of plots in figure 4 and this estimation, it is quite plausible that a transverse exponent λ_{\perp} of the $O(10)$ model is somewhat larger than that of the $O(4)$ model. It is consistent

with the idea that $2 - \lambda_{\perp}$ decreases for large n and tends to zero at $n \rightarrow \infty$. This behavior is fully consistent with the predictions of [8], but not so well consistent with the standard theory, according to which λ_{\perp} is always 2 and, therefore, $\Delta\lambda_{\perp} = 0$ is expected. According to our estimates $(\lambda_{\perp})_{n=10} = 1.9723(90)$ and $\Delta\lambda_{\perp} = 0.0121(52)$, we have $\lambda_{\perp} = 1.960(10)$ for $n = 4$. It perfectly agrees with our earlier estimate $\lambda_{\perp} = 1.955 \pm 0.020$ [16].

4. The ratio universality test

We have extended the MC analysis of our earlier data [16] for the $O(4)$ model at two different couplings, $\beta = 1.1$ and $\beta = 1.2$, to test the expected (according to [8]) universality of the ratio bM^2/a^2 , discussed already in the end of section 1. According to (1.5), (1.6) and (1.8), the universality of bM^2/a^2 implies that the quantity

$$R(\mathbf{k}) = \frac{k^{-d} M^2 G_{\parallel}(\mathbf{k})}{G_{\perp}^2(\mathbf{k})} \quad (4.1)$$

tends to some universal constant at $k \rightarrow 0$, i. e., $\lim_{k \rightarrow 0} R(\mathbf{k}) = bM^2/a^2$. We have tested this property by comparing the $R(k)$ plots at $\beta = 1.1$ and $\beta = 1.2$, where $R(k) \equiv R(|\mathbf{k}|)$ in the $\langle 100 \rangle$ direction. Note that the quantities in (4.1) are determined in the thermodynamic limit at $h = +0$. We have verified that this limit is practically (within the statistical error bars) reached within $k \geq k_{14}$ (where $k_{\ell} = 2\pi\ell/350$) for the largest lattice size $L = 350$ and the smallest external fields $h = 0.0003125$ and $h = 0.0004375$ at which simulations were performed. The estimates of spontaneous magnetization obtained in [8], i.e., $M = 0.484475(48)$ at $\beta = 1.1$ and $M = 0.560178(40)$ at $\beta = 1.2$, are used here. The calculated plots are depicted in figure 5. The results for both $h = 0.0003125$ and $h = 0.0004375$ are available at $\beta = 1.1$. As we can see from figure 5, the corresponding two plots of $R(k)$ (solid circles and diamonds) lie practically on top of each other, indicating that the finite- h effects are negligibly small. The range $h \geq 0.0004375$ is considered for $\beta = 1.2$ in [16]. Fortunately, the finite- h effects at $\beta = 1.2$ are similar to those at $\beta = 1.1$, so that the estimate of $R(k)$ at $h = 0.0004375$ is valid at $\beta = 1.2$. The corresponding plot (empty circles) in figure 5 slightly deviates from the two plots at $\beta = 1.1$. However, all three plots merge within the statistical error bars at the smallest wave vector magnitudes k considered here. This confirms the expected universality of the ratio bM^2/a^2 . The plot of empty circles in figure 5 apparently saturates at a value about 0.166 for small wave vectors. Taking into account the two other plots, we can judge that $0.16 < R(0) < 0.18$ most probably holds for the asymptotic value $R(0) = \lim_{k \rightarrow 0} R(k)$. Thus, we have an estimate $R(0) = 0.17 \pm 0.01$.

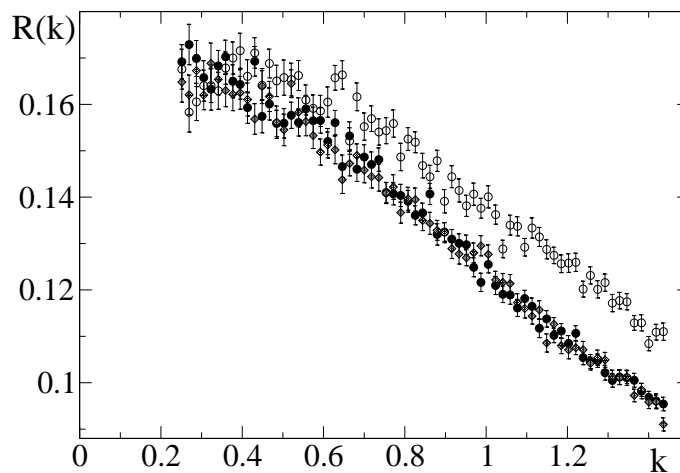


Figure 5. The $R(k)$ plots of the 3D $O(4)$ model, evaluated from the MC data for the lattice of size $L = 350$ at $\beta = 1.1$ and $h = 0.0003125$ (solid circles), $\beta = 1.1$ and $h = 0.0004375$ (diamonds), as well as at $\beta = 1.2$ and $h = 0.0004375$ (empty circles).

5. Spontaneous magnetization

We estimated the spontaneous magnetization of the 3D $O(10)$ model at $\beta = 3$ based on our magnetization data $M(h, L)$ depending on h and L . We observed a rather fast convergence to the thermodynamic limit, e. g., $M(h_{\min}, L) = 0.31658(46), 0.45286(23), 0.470839(90), 0.471959(38), 0.472151(23), 0.472148(16)$ at $L = 32, 64, 128, 192, 256$ and 350 , respectively. According to this, we can take the largest- L value as a good approximation for $M(h_{\min}) = \lim_{L \rightarrow \infty} M(h_{\min}, L)$. Using this method, we obtained $M(h_{\min}) = 0.472148(16)$, $M(2h_{\min}) = 0.4742786(98)$ and $M(4h_{\min}) = 0.4772753(76)$. According to (1.4), we fit these data to the ansatz $M(h) = M(+0) + a_1 h^\rho$ with $\rho = 0.5211(69)$, evaluated from (1.9) by inserting here $\lambda_\perp = 1.9723(90)$ obtained in section 3. It yields $M \equiv M(+0) = 0.467343(99)$. Assuming the standard-theoretical value $\rho = 1/2$, we obtain $M = 0.467030(26)$. Fits to a refined ansatz $M(h) = M(+0) + a_1 h^\rho + a_2 h$ yield $M = 0.46711(14)$ at $\rho = 0.5211(69)$ and $M = 0.46696(14)$ at $\rho = 1/2$. Since we have only three data points for $M(h)$, this can be considered as a raw estimation yielding $M \approx 0.467$. However, this estimation is accurate enough to see that $\beta = 3$ corresponds to the ordered phase with $M > 0$.

6. Conclusions

In the actual work, the previous MC studies [10, 16] of the transverse and longitudinal correlation functions in the 3D $O(n)$ models with $n = 2$ and $n = 4$ have been extended, including the $n = 10$ case (sections 2 and 3). It gives us an important information about the behavior of the exponent λ_\perp at large n . According to our MC analysis, a self-consistent (within the standard theory) estimation of λ_\perp for $n = 10$ shows a small deviation from the standard-theoretical prediction $\lambda_\perp = 2$, yielding $\lambda_\perp = 1.9723(90)$ (section 3). The fact that this deviation is quite small can be well understood, since $\lambda_\perp \rightarrow 2$ is expected at $n \rightarrow \infty$ according to the known results for the spherical model, corresponding to this limit. Comparing the plots of the effective transverse exponent at $n = 10$ and $n = 4$, it has been stated that these plots are surprisingly similar, i. e., only slightly shifted with respect to each other. The estimation of this shift suggests that the transverse exponent for $n = 10$ is larger than that for $n = 4$ by an amount of $\Delta\lambda_\perp = 0.0121(52)$ (section 3). It is consistent with the idea that $2 - \lambda_\perp$ decreases for large n and tends to zero at $n \rightarrow \infty$. We have also verified and confirmed the expected universality of the ratio bM^2/a^2 for the $O(4)$ model by analyzing the correlation functions at two different couplings, i. e., $\beta = 1.1$ and $\beta = 1.2$ (section 4).

The actual MC results are fully consistent with the predictions of the GFD theory [8] (see section 1) and not so well consistent with the standard theory, according to which λ_\perp is always 2.

Acknowledgements

This work was made possible by the facilities of the Shared Hierarchical Academic Research Computing Network (SHARCNET:www.sharcnet.ca). It has been performed within the framework of the ESF Project No. 1DP/1.1.1.2.0/09/ APIA/VIAA/142, and with the financial support of this project. R. M. acknowledges the support from the NSERC and CRC program.

References

1. Lawrie I.D., J. Phys. A, 1981, **14**, 2489; doi:10.1088/0305-4470/14/9/041.
2. Lawrie I.D., J. Phys. A, 1985, **18**, 1141; doi:10.1088/0305-4470/18/7/021.
3. Hasenfratz P., Leutwyler H., Nucl. Phys., 1990, **B343**, 241; doi:10.1016/0550-3213(90)90603-B.
4. Täuber U.C., Schwabl F., Phys. Rev. B, 1992, **46**, 3337; doi:10.1103/PhysRevB.46.3337.
5. Schäfer L., Horner H., Z. Phys. B, 1978, **29**, 251; doi:10.1007/BF01321190.
6. Anishetty R., Basu R., Hari Dass N.D., Sharatchandra H.S., Int. J. Mod. Phys. A, 1999, **14**, 3467; doi:10.1142/S0217751X99001615.
7. Dupuis N., Phys. Rev. E, 2011, **83**, 031120; doi:10.1103/PhysRevE.83.031120.
8. Kaupužs J., Prog. Theor. Phys., 2010, **124**, 613; doi:10.1143/PTP.124.613.

9. Kaupužs J., Rimšāns J., Melnik R.V.N., Ukr. J. Phys., 2011, **56**, 845.
10. Kaupužs J., Can. J. Phys., 2012, **9**, 373; doi:10.1139/p2012-028.
11. Dimitrović I., Hasenfratz P., Nager J., Niedermayer F., Nucl. Phys., 1991, **B350**, 893; doi:10.1016/0550-3213(91)90167-V.
12. Engels J., Mendes T., Nucl. Phys. B, 2000, **572**, 289; doi:10.1016/S0550-3213(00)00046-8.
13. Engels J., Holtman S., Mendes T., Schulze T., Phys. Lett. B, 2000, **492**, 219; doi:10.1016/S0370-2693(00)01079-0.
14. Engels J., Vogt O., Nucl. Phys. B, 2010, **832**, 538; doi:10.1016/j.nuclphysb.2010.02.006.
15. Kaupužs J., Melnik R.V.N., Rimšāns J., Commun. Comput. Phys., 2008, **4**, 124.
16. Kaupužs J., Melnik R.V.N., Rimšāns J., Phys. Lett. A, 2010, **374**, 1943; doi:10.1016/j.physleta.2010.03.002.
17. Wolff U., Phys. Rev. Lett., 1989, **62**, 361; doi:10.1103/PhysRevLett.62.361.
18. Pearce P.A., Thompson C.J., J. Stat. Phys., 1977, **17**, 189; doi:10.1007/BF01040101.

Сингулярності голдстоунівських мод в $O(n)$ моделях

Я. Каупуцс^{1,2}, Р.В.Н. Мельнік³, Я. Рімсанс^{1,2}

¹ Інститут математики та комп'ютерних наук, Університет Латвії,
бульвар Я. Райніса, 29, LV-1459 Рига, Латвія

² Інститут математичних наук та інформаційних технологій, Університет м. Лієпая,
вул. Лієла, 14, LV-3401 Лієпая, Латвія

³ Університет ім. Вільфреда Лорье, Ватерлоо, Онтаріо, Канада, N2L 3C5

У тривимірних $O(n)$ моделях з $n = 2, 4, 10$ здійснено аналіз методом Монте Карло (МК) сингулярностей голдстоунівських мод для поперечної і поздовжньої кореляційних функцій, які поводять себе як $G_{\perp}(\mathbf{k}) \simeq ak^{-\lambda_{\perp}}$ і $G_{\parallel}(\mathbf{k}) \simeq bk^{-\lambda_{\parallel}}$ у впорядкованій фазі при $k \rightarrow 0$. Нашою метою є перевірити цікаві теоретичні передбачення, згідно яких індекси λ_{\perp} і λ_{\parallel} є нетривіальними ($3/2 < \lambda_{\perp} < 2$ і $0 < \lambda_{\parallel} < 1$ у трьох вимірах) і коефіцієнт bM^2/a^2 (де M є спонтанною намагніченістю) є універсальний. Тривіальні стандартні теоретичні значення є $\lambda_{\perp} = 2$ і $\lambda_{\parallel} = 1$. Наш попередній МК аналіз дає $\lambda_{\perp} = 1.955 \pm 0.020$ і λ_{\parallel} приблизно рівне 0.9 для $O(4)$ моделі. Недавня МК оцінка λ_{\parallel} , яка допускає поправки для скейлінга стандартної моделі, дає $\lambda_{\parallel} = 0.69 \pm 0.10$ для $O(2)$ моделі. Тепер ми здійснили подібну МК оцінку для $O(10)$ моделі, яка дає $\lambda_{\perp} = 1.9723(90)$. Ми побачили, що графік ефективного поперечного індекса для $O(4)$ моделі є систематично зсунутий вниз по відношенню до графіка для $O(10)$ моделі на $\Delta\lambda_{\perp} = 0.0121(52)$. Це узгоджується з думкою, що $2 - \lambda_{\perp}$ зменшується для великих n і прямує до нуля при $n \rightarrow \infty$. Ми також перевірили і підтвердили очікувану універсальність bM^2/a^2 для $O(4)$ моделі, для якої було здійснено симуляції при двох різних температурах.

Ключові слова: моделювання Монте Карло, n -компонентні векторні моделі, кореляційні функції, сингулярності голдстоунівських мод